3.3

DIAGNOSTIC TESTING IN THE EVALUATION OF CMAQ AGAINST OBSERVATIONS FROM SOS FIELD INTENSIVES

J.R. Arnold* and Robin L. Dennis
Atmospheric Sciences Modeling Division
Air Resources Laboratory
National Oceanic and Atmospheric Administration

on assignment to

National Exposure Research Laboratory
Office of Research and Development
U.S. Environmental Protection Agency
Research Triangle Park, NC 27705 USA

jra@hpcc.epa.gov, rdennis@hpcc.epa.gov

Voice 206.553.8579 (jra) Fax 206.553.8210

1. INTRODUCTION

We have previously described a model evaluation methodology that distinguishes several types of model testing (Arnold, *et al*., 1998). Two components of that methodology are operational testing to judge the performance and overall behavior of a model over specific attributes, and diagnostic testing to help reveal potential compensating errors in model inputs or processing.

Diagnostic testing of a model is *in situ* testing of model components using data that emphasize atmospheric processes, often with mass balance techniques, special species ratios, and process and reaction rate information not typically stored in model output. We have developed new diagnostic probes through process-oriented studies using theoretical assumptions, model-derived explanations, and results from instrumented models ranging from 1-D box models to the full 3-D photochemical modeling system (see Tonnesen and Dennis, 2000a and 2000b).

One listing of diagnostic measures to probe the chemistry of O_3 production ($P(O_3)$) in the atmosphere and in model mechanisms looks like this:

- Individual Components Aspects: Radical Initiation and Termination, Competition Among Radical Termination Pathways, and Air Mass Aging
- Process Aspects: OH Production, Radical Propagation and Propagation Efficiency, OH and NO_X Chain Length, $P(O_3)$ Efficiency per NO_X Termination
- Response Surface Aspects: System State Relative to the O_3 Ridgeline, Location of the Ridgeline in Response Space, Slope of the Radical-limited Response Surface, Slope of the NO_X-limited Response Surface

The first category of individual components includes initiation of new radicals from O_3, HCHO, and HONO, and termination of radical cycling either as peroxy radicals self-combine and/or OH and NO_2 are converted to NO_Z ($NO_Z = NO_Y - NO_X$).

The second category of photochemical process groupings includes propagation of radicals through the system as HO_2 radicals are formed and convert NO to NO_2, and the related concepts of OH propagation efficiency (Pr_{OH}) and chain length. Pr_{OH} is defined as the average fraction of OH re-created over one cycle of OH reactions. The OH chain length is defined as the average number of times a new radical cycles through the system before being removed in a termination reaction; a companion cycle with a similarly defined chain length is set up with the conversion of NO to NO_2 in which NO is re-created and cycled before being terminated.

The third category includes elements of the integrated response of a photochemical system such as that represented on a typical response surface of the O_3 mixing ratio ($[O_3]$) as shown in Figure 1.

Tests of this third type probe a model's ability to track systemic change and typically involve species and the ratios of species believed to correlate consistently with the VOC- and NO_X-sensitive $P(O_3)$, often referred to as "indicators" of control strategy sensitivity. These measures of the sensitivity of O_3 to NO_X and VOC changes are characteristics of specific photochemical systems in that each system may have particular combinations of

* *Corresponding author address:* J.R. Arnold, NOAA / USEPA ASMD, 1200 6th Avenue / 9th Fl / OEA-95, Seattle, WA 98101-1128

NO_X and VOCs that determine its position on the O_3 response surface in one region or the other relative to the $[O_3]$ ridgeline. However, we have observed in the model that individual systems exhibit marked diurnal behavior, too, moving from strongly radical-limited in the morning to the transition state near the $[O_3]$ ridgeline and into the NO_X-limited region of the response surface later in the day. Tracking this air mass history with cumulative diagnostic tests is important for understanding the model's behavior for its intended use in control strategy development and assessment since the position of a photochemical system in one or the other regions of the response surface determines whether VOC or NO_X controls are to be preferred.

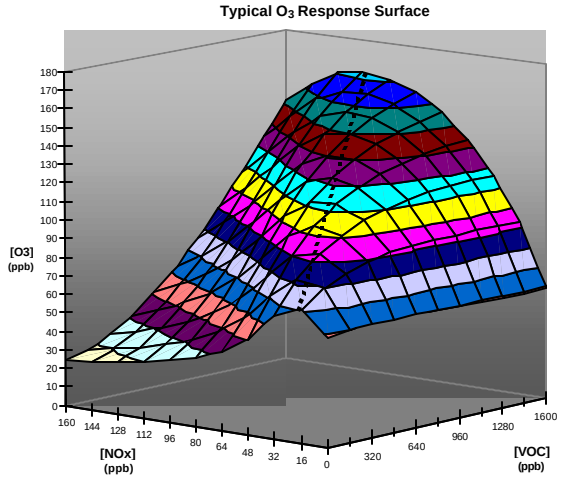

Figure 1. Nonlinear $[O_3]$ response surface for changes in initial NO_X and VOC, indicating regions of radical and NO_X sensitivities and the ridgeline (heavy dotted line here) of maximum $[O_3]$ between them.

2. EXPERIMENTAL

The 1995 Southern Oxidant Study Nashville / Middle Tennessee Ozone Study (SOS 95) included comprehensive air quality field experiments on multiple aircraft platforms and at several highly-instrumented surface sites in and around the city of Nashville (see Meagher, *et al*. (1998) for the study overview). Our diagnostic testing has focused on continuous O_3, NO, precise and specific NO_2, and total NO_Y measurements at three of the "level 2" and "level 3" sites: Dickson, ~60 km west of Nashville and designated an urban-suburban chemistry site by SOS 95 study planners but one strongly influenced by large point sources including the Cumberland and Johnsonville power plants; Giles, ~150 km south of Nashville and designated a regional chemistry site, though one having previously unexpected local NO_X sources as well; and Youth, ~25 km southeast of Nashville and designated a site for urban-suburban chemistry. Figure 2 shows a map of chemistry sites and local sources in the SOS95 domain. Fuller description of the configuration of these sites and experimental details of the data collection are given in Olszyna, *et al*. (1998).

We report here from a CMAQ modeling series for 5-18 July 1995, a two-week period that includes both the highest $[O_3]$ of the six-week SOS 95 field intensive and several days with low $[O_3]$ maxima that follow frontal passage clean out of the atmosphere. CMAQ was run with 21 vertical layers in domains with 36 km, 12 km, and 4 km horizontal grid squares. CB4 and RADM2 chemistries were each run with the SMVGear solver. Additional details of model parameterizations and setup are given in Arnold *et al*. (2002).

3. RESULTS AND DISCUSSION

Space limitations restrict this abstract to a discussion of the urban-suburban chemistry site in SOS95, Youth; additional results from comparisons at other sites will appear in the presentation.

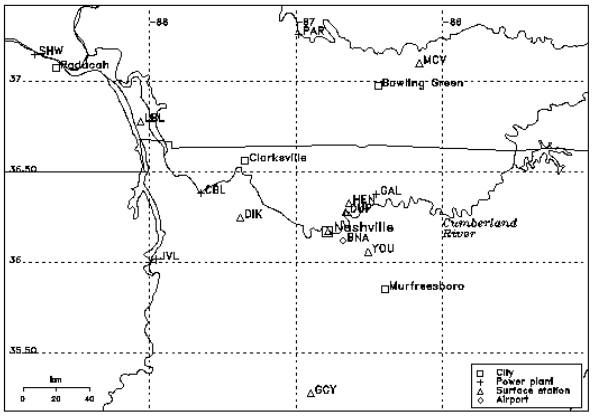

Figure 2. Map of the SOS95 surface sites Dickson (DIK), Giles (GCY), and Youth (YOU), urban areas, and nearby power plants Cumberland (CBL), Johnsonville (JVL), and Gallatin (GAL). From Senff, *et al*., (1998).

3.1 Response Surface Probe : $[O_3]$ / $[NO_X]$

The ratio $[O_3]/[NO_X]$ has been shown with work in Eulerian models to be a reliable indicator of the O_3 sensitivity of a photochemical system as characterized by its position on the $[O_3]$ response surface relative to the ridgeline (Tonnesen and Dennis, 2000a and 2000b). Values of the indicator <15 indicate the strongly radical-limited, NO_X-inhibited, and hence VOC-sensitive, conditions often prevalent at the surface in the early morning or in fresh power plant plumes. Values >46 indicate a position across the $[O_3]$ ridgeline well into the NO_X-limited, and hence NO_X-sensitive, region and outside the effects of fresh power plant plumes. Using observations at the three SOS 95 sites, the ridgeline

generally falls in a range between 15 and 25 but can vary day-to-day and site-to-site.

Figure 3 shows a histogram of all hours for which there were observations at Youth binned for ranges at the radical-limited and the NO_X-limited extremes and near the $[O_3]$ ridgeline.

For the most part, CMAQ correctly reproduces the distributions of the observed indicator values across the different conditions represented at this site. Discrepancies in the >46 range are smaller with the 4 km models than with the 12 km which appear to have a ceiling related to excessive NO_X retained through the end of the day that is not apparent at the finer grid spacing. Here at Youth, where photochemistry is dominated by more typical aged urban plumes, the probe shows that the 4 km models tend to perform better than the 12 km, predicting a more appropriate number of hours each day with an indicator value >46, for example. This result for the indicator probe is consistent with other performance measures showing better operational performance by the 4 km models (Arnold and Dennis, 2001). Finally, differences between the chemistries are not readily apparent with this test.

We interpret these results with those from other SOS95 sites to mean that the model's photochemical

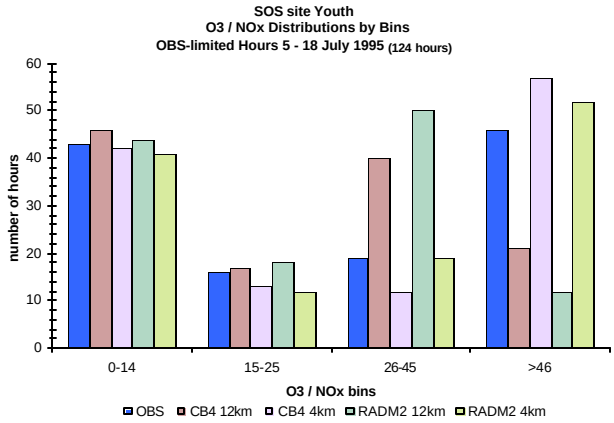

Figure 3. Ridgeline indicator distribution for observations and models at Youth.

processing as indicated by the ratio $[O_3]/[NO_X]$ changing as the photochemical system changes state and moves over the response surface is appropriately reproducing changes of the atmosphere.

3.2 Individual Components Probe : $[NO_Z]$ / $[NO_Y]$

The age of an air mass can usefully be represented as the fraction of NOY which has been converted to NO_Z. Values of $[NO_Z]/[NO_Y]$ <0.6 indicate a fresher NO_X plume with an increased potential for O_3 production or loss, conditional on radical availability, *i.e.*, the system's position on the response surface; values >0.6, then, indicate an aged air mass with less potential for change in $[O_3]$.

Figure 4 shows a diurnal time plot of the $[NO_Z]/[NO_Y]$ ratio at Youth where the model (RADM2 chemistry in this example) reproduces the daily curve quite well, tracking both the low values of fresher NO_X and the higher values of more processed NO_Z correctly through the photochemical day.

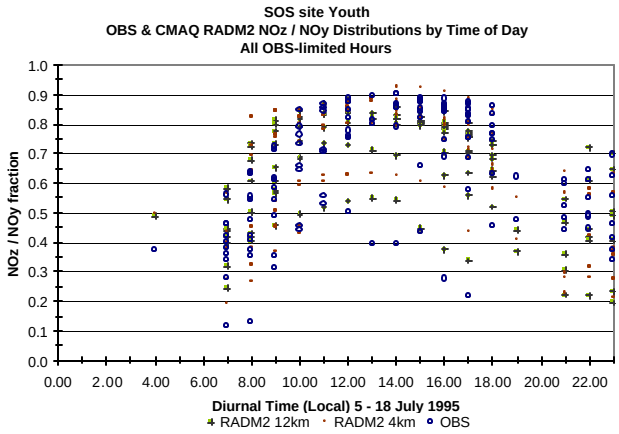

Figure 4. Photochemical age fraction for each hour every day, RADM2 chemistry at Youth.

We interpret the result from this individual components probe, that the models have NO_X processing reactions and rates substantially similar to those in the atmosphere, is consistent with the information from our ridgeline indicator probe described above and so increases our confidence that the model's process representations are largely correct and complete.

An additional utility of our diagnostic probes is using them together with one as a filter of these complex atmospheric processes. So, for example, Figure 5 shows $[O_3]$ (RADM2 chemistry only) plotted as a function of the aging fraction $[NO_Z]/[NO_Y]$ and filtered by a $[O_3]/[NO_X]$ value >46. Filtering in this way ensures that only the most NO_X-limited hours of the strongly-varying photochemical day are included.

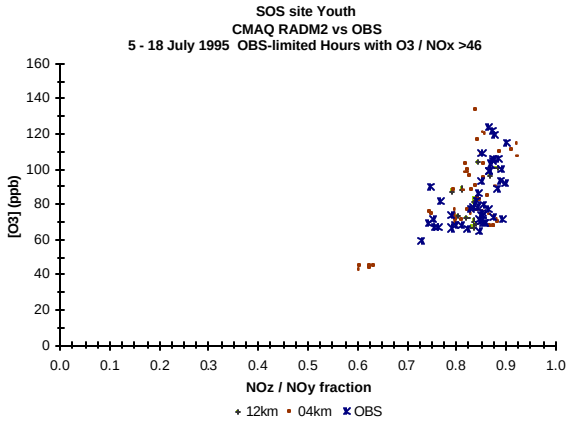

Figure 5. $[O_3]$ as a function of air mass age for the NO_X-limited conditions indicated by $[O_3]/[NO_X]$ >46, RADM2 chemistry at Youth.

Filtered in this way, the plot suggests that for hours in the strongly NO_X-limited region of the response surface, where precursor control would be intended to work on final maximum $[O_3]$, the model appears to be aging NOX to NOZ – along one pathway – and producing O3 – along another – appropriately.

3.3 Process Diagnostics probe : [O3] vs. [NOZ]

The slope of the line produced by plotting $[O_3]$ against $[NO_Z]$ is a measure of the photochemical processing of NO_X referred to as the O_3 production efficiency, or the number of O_3 molecules produced for each NO_X processed to NO_Z. In this way the relation indicates a cumulative $P(O_3)$ rate and the average NO_X chain length over an air mass history.

In the past this relation has been presented with observations or model data for all hours either observed or in the simulation. However, using all hours complicates interpretation of the test for either observations or the model and should be avoided. The complication arises from mixing together rates from very different parts of the diurnal O_3 production cycle which is determined by the relative availabilities of NO_X and radicals changing through time as the system migrates over the O_3 response surface.

To sharpen interpretation of this process diagnostic test, we again select hours in the observations and the model filtered by the ridgeline indicator for the $[O_3]/[NO_X]$ range >46 which ensures that the system is well out of the radical-sensitive region, not contaminated by large fresh NO_X plumes, and significantly across the ridgeline into the NO_X-limited region of the response surface.

Figure 6 shows that CMAQ does credibly well reproducing the curve of $P(O_3)$ to $P(NO_Z)$ at the near-urban Youth site, tracing a line very similar to that of the observations in slope and intercept.

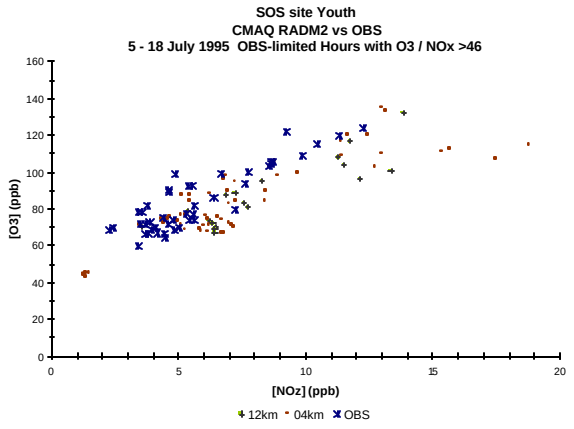

Figure 6. $[O_3]$ as a function of NO_Z for the NO_X-limited conditions indicated by $[O_3]/[NO_X]$ >46, RADM2 chemistry at Youth.

We interpret this information to be consistent with that from our other probes of NO_X processing: that CMAQ is for the most part converting NO_X to NO_Z and producing O_3 in a manner very similar to that of the atmosphere in the near-urban conditions at Youth.

4. SUMMARY

The three probes discussed here provide robust and reliable process information chiefly about the aggregate production rate of O_3 and the details of NO_X cycling in determining that rate. Importantly, the three probes give consistent information about the model processes and are particularly useful when used together. For example, the response surface ridgeline indicator $[O_3]/[NO_X]$ can broadly characterize a photochemical system: low values of the ratio tend to be associated with early morning periods when $[NO_X]$ is high and $[O_3]$ low, and higher values of the ratio are associated with hours late in the photochemical day when conditions have reversed. However, the values of this ratio are not uniquely determined and could be ambiguous with regard to the response surface ridgeline if the systems were not also filtered by an indicator of air mass aging, the fraction NO_Z/NO_Y, for example. In a similar way, information about the production efficiency of O_3 per NO_X converted, the slope of the line of O_3 to NO_Z, is sharpened significantly when filtered by the ridgeline indicator to be centered in the region of strongest NO_X limitation. Thus the power of each indicator can be exploited more fully when applied together for building interpretations of atmospheric processes in the observations and in the model.

5. REFERENCES

Arnold, J. R., Dennis, R. L., 2001. First results from operational testing of the U.S. EPA Models-3 / Community Multiscale Model for Air Quality (CMAQ). In: Gryning, S.-E., Schiermeier, F. A. (Eds.), Air Pollution Modeling and Its Application XIV. Kluwer Academic, Dordrecht.

Arnold, J. R., Dennis, R. L., Tonnesen, G. S., 1998. Advanced techniques for evaluating Eulerian air quality models: background and methodology. In: American Meteorological Society 10th Joint Conference on the Applications of Air Pollution Meteorology with the American Waste Management Association, pp. 1-5. American Meteorological Society, Boston.

Arnold, J. R., Dennis, R. L., Tonnesen, G. S., 2002. Diagnostic Evaluation of Numerical Air Quality Models with Specialized Ambient Observations: Testing CMAQ at Selected SOS95 Ground Sites. Atmospheric Environment. (submitted).

Meagher, J. F., Cowling, E. B., Fehsenfeld, F. C., Parkhurst, W. J., 1998. Ozone formation and transport in the southeastern United States: Overview of the SOS Nashville/Middle Tennessee Ozone Study. Journal of Geophysical Research 103, 22213-22223.

Olszyna, K. J., Parkhurst, W. J., Meagher, J. F., 1998. Air chemistry during the 1995 SOS/Nashville intensive determined from level 2 network. Journal of Geophysical Research 103, 31143-31153.

Senff, C. J., Hardesty, R. M., Alvarez II, R. J., Mayor, S. D., 1998. Airborne lidar characterization of power plant plumes during the 1995 Southern Oxidants Study. Journal of Geophysical Research 105, 31173-31189.

Tonnesen, G. S., Dennis, R. L., 2000a. Analysis of radical propagation efficiency to assess ozone sensitivity to hydrocarbons and NOx. Part I: Local indicators of instantaneous odd oxygen production sensitivity. Journal of Geophysical Research 105, 9213-9225.

Tonnesen, G. S. Dennis, R. L., 2000b. Analysis of radical propagation efficiency to assess ozone sensitivity to hydrocarbons and NOx. Part II: Long-lived species as indicators or ozone concentration sensitivity. Journal of Geophysical Research 105, 9227-9241.